Title

Segmental isotope analysis of the vertebral centrum reveals the spatiotemporal population structure of adult Japanese flounder *Paralichthys olivaceus* in Sendai Bay, Japan

Authors

Yoshikazu Kato[1,2], Hiroyuki Togashi[3], Yutaka Kurita[3], Yutaka Osada[1,4], Yosuke Amano[5,6], Chikage Yoshimizu[1], Hiromitsu Kamauchi[1,7], Ichiro Tayasu[1]

[1] Research Institute for Humanity and Nature, 457-4 Motoyama, Kamigamo, Kita-ku, Kyoto 603-8047, Japan

[2] Graduate school of Environmental Studies, Nagoya University, Furo-cho, Chikusa-ku, Nagoya, Aichi 464-8601, Japan

[3] Shiogama Field Station, Fisheries Resources Institute, Japan Fisheries Research and Education Agency, 3-27-5 Shinhama-cho, Shiogama, Miyagi 985-0001, Japan

[4] Yokohama Field Station, Fisheries Resources Institute, Japan Fisheries Research and Education Agency, 2-12-4 Fukuura, Kanazawa, Yokohama, Kanagawa 236-8648, Japan

[5] Tohoku National Fisheries Research Institute, Japan Fisheries Research and Education Agency, 3-27-5 Shinhama-cho, Shiogama, Miyagi 985-0001, Japan

19 [6] Fukushima Prefectural Fisheries and Marine Science Research Centre, 13-2, Onahama-Shimokajiro,

20 Iwaki, Fukushima 970-0316, Japan

21 [7] Nagoya, Aichi, Japan

22

23 **Corresponding author**

24 Yoshikazu Kato

25 Graduate school of Environmental Studies, Nagoya University

26 Furo-cho, Chikusa-ku, Nagoya, Aichi 464-8601, Japan

27 E-mail: yoshikatoo@gmail.com

28

29 **Acknowledgments**

30 We are grateful to Y. Tanaka and K. Yamamoto for assistance with sample treatment. We thank T. Nakano,

31 K.C. Shin, Y. Saitoh, J. Matsubayashi, K. Shirai, and N. Okuda for useful comments in the course of this

32 study. We also appreciate two anonymous reviewers helped to improve the manuscript.

Abstract

To identify the origin of various fishes and reconstruct their migration history at the individual level, isotope analysis is a powerful alternative to artificial tagging. We used a novel individual-based methodology to reconstruct individual migratory and/or trophic shifts associated with growth based on isotopic data in the vertebral centrum of adult Japanese flounder *Paralichthys olivaceus* in Sendai Bay. We measured carbon and nitrogen isotope ratios ($\delta^{13}C$ and $\delta^{15}N$) in muscle tissues, and conducted a segmental isotope analysis of bulk $\delta^{13}C$ ($\delta^{13}C_{bulk}$), bulk $\delta^{15}N$ ($\delta^{15}N_{bulk}$), and $\delta^{15}N$ of glutamic acid ($\delta^{15}N_{Glu}$) and phenylalanine ($\delta^{15}N_{Phe}$) in vertebral collagen. The $\delta^{15}N_{Glu}$ and $\delta^{15}N_{Phe}$ values for bone collagen revealed an increase in trophic position and a shift to lower trophic baselines ($\delta^{15}N_{Base}$: indicative of $\delta^{15}N$ values of primary trophic sources) for most individuals. For both $\delta^{13}C_{bulk}$ and $\delta^{15}N_{bulk}$, we detected significant positive correlations between values for muscle and the outermost section of vertebral collagen. A nonlinear time-series analysis of $\delta^{13}C_{bulk}$ and $\delta^{15}N_{bulk}$ suggested that a combination of intrinsic (the timing of migration from the nursery to deep offshore areas in juveniles) and extrinsic (habitat and/or food qualities) factors influence the isotopic chronology. A segmental isotope analysis revealed the segregation of individuals among sampling sites at all life stages and changes in trophic positions and $\delta^{15}N_{Base}$ values during growth. Our results suggest that the *P. olivaceus* population in Sendai Bay has both temporal and spatial structure. The temporal structure may be caused by variation in the timing of migration from the nursery to the deep offshore area in juveniles, and the spatial structure may be

explained by individual variation in habitat preferences.

Funding

This work was supported by the CREST program of the Japan Science and Technology Agency (grant number JPMJCR13A3), the Japan Society for the Promotion of Science (KAKENHI grant number 16H02524), and the Stock Assessment Program of the Japan Fisheries Research and Education Agency and Fisheries Agency.

Conflicts of interest/Competing interests

The authors declare that they have no known competing financial interests or personal relationships that could have appeared to influence the work reported in this paper.

Ethics approval

All fish captures and handling were conducted in accordance with the guidelines of concerned government ministries in Japan.

Consent to participate

Not applicable

Consent for publication

Not applicable

Availability of data and material (data transparency)

Not applicable

Code availability (software application or custom code)

Not applicable

Authors' contributions

I.T. and Y. Ku. conceived the study; H.T., Y. Ku., Y.A., C.Y., H.K., and Y. Ka. collected the data; and H.T., Y. Ka., H.K., and Y.O. analyzed the data. Y. Ka. and Y.O. wrote the first draft of the manuscript, and all authors contributed substantially to the revisions.

Introduction

In marine ecology and fisheries, it is quite challenging to quantify the scale and magnitude of individual migration across life-history stages or mixing among populations (Cowen et al. 2006). Tracking the movement of individuals over their lifetime is the ideal approach for this purpose. This can be achieved by artificial tagging (Mellon-Duval et al. 2010) or telemetry (Cooke et al. 2011; Brownscombe et al. 2019). Alternatively, isotope analysis of otolith bulk tissue is a powerful tool (Gao and Bean 2008, Bradbury et al. 2011, Wells et al. 2015, Fraile et al. 2016). The otolith bulk tissue of teleost fishes is composed mostly of calcium carbonate (Campana 1999), and isotopic information for the juvenile period is preserved near the central region. For example, wild and stocked individuals during the juvenile stage have been successfully discriminated based on otolith stable isotope ratios in lake trout (*Salvelinus namaycush*: Schaner et al. 2007), pink salmon (*Oncorhynchus gorbuscha*: Tomida et al. 2014), and Japanese eel (*Anguilla japonica*: Kaifu et al. 2018).

Generally, carbon and nitrogen isotope ratios (δ^{13}C and δ^{15}N) are useful for assessing the migration and ecological connectivity of fish species (Cook et al. 2007, Rodgers and Wing 2008, Green et al. 2012). With respect to trophic relationships, δ^{13}C and δ^{15}N analyses are based on four fundamental assumptions. First, primary producers show unique isotopic signatures that depend on the physiology of the producer and the geochemical environment (Maberly et al. 1992). Second, consumers fractionate the carbon and nitrogen isotopes of foods in predictable ways (DeNiro and

101 Epstein 1978, 1981) specific to taxonomic and functional feeding groups (Vanderklift and Ponsard 2003).
102 Third, isotopic signatures of consumers reflect the mass balance of assimilated foods, enabling estimation
103 of the relative contributions of multiple food sources with a mixing model (Phillips et al. 2005, Moore
104 and Semmens 2008). Fourth, stable isotope analysis can integrate dietary information over time periods
105 from weeks to years, depending on the body size and turnover rate. In addition to the common usage of
106 muscle for $\delta^{13}C$ and $\delta^{15}N$ analyses in fishes, bone collagen also provides insight into the foraging ecology
107 and habitat use of marine vertebrates (Schoeninger and DeNiro 1984, Tomaszewicz et al. 2016).
108 However, the temporal resolution of isotopic values obtained from whole bone collagen is low because
109 the turnover time is longer than that of other tissues, such as muscle and liver tissues (Sholto-Douglas &
110 Field 1991, Gaston & Suthers 2004) (note that growth-based turnover in bone collagen is quite faster in
111 some cases: Ankjærø et al. 2012). Furthermore, recent researches suggested that $\delta^{15}N$ values recorded in
112 the sclerochronological layers of the otoliths can be used to determine the trophic levels, food sources and
113 diet changes of fish (Grønkjær et al. 2013; Shiao et al. 2018).
114 Comparing with previous tracking methods, i.e., the tagging, telemetry, and otolith isotope analysis,
115 segmental isotope analysis of collagen in vertebrae of teleost fishes has the potential to obtain not only
116 successional information of movement trajectory but also that on trophic shift (or stability) of individual
117 fish along with their growth (especially, it is quite advantageous to obtain the information during the
118 period of tiny juveniles). Previous research showed that the method can detect dietary isotopic shifts in

feeding experiments (Matsubayashi et al. 2019). Because the cone-shaped vertebral centrum grows radially, similar to the growth rings of an otolith or a tree, chronological changes in isotopic signatures are preserved from the apex to the outermost edge, allowing for the reconstruction of isotopic shifts resulting from changes in diet and/or habitat over time (Kerr et al. 2006; Estrada et al. 2016; Matsubayashi et al. 2017). Bone collagen is quite effective than otoliths for tracking individual fish in isoscapes because it provides spatially explicit descriptions and predictions of isotopic values across a landscape (West et al. 2008, Bowen 2010), especially for trophic relationships revealed by elements that are scarce in otoliths (e.g., $\delta^{15}N$ and $\delta^{34}S$: Doubleday et al. 2018).

In addition to the usability of $\delta^{13}C$ and $\delta^{15}N$ of bulk tissue ($\delta^{13}C_{bulk}$ and $\delta^{15}N_{bulk}$), the availability of $\delta^{15}N$ in bone collagen also expands the scope of ecological analysis by allowing compound-specific $\delta^{15}N$ analysis such as amino acids ($\delta^{15}N_{AA}$) (Chikaraishi et al. 2009; Ishikawa et al. 2014; Matsubayashi et al. 2020). The estimation of trophic positions (TP) using $\delta^{15}N_{AA}$ has several advantages (Chikaraishi et al. 2009; Ohkouchi et al. 2017). First, the TP is estimated from two amino acids and it is not necessary to determine isotopic values of primary producers to estimate the TP of consumers. Second, $\delta^{15}N_{AA}$ values of consumers reflect integrated values of primary producers that have actually contributed to them in the food web. Third, the method with $\delta^{15}N_{AA}$ is also applicable to clarify food-web structures in both aquatic and terrestrial ecosystems (Chikaraishi et al. 2010, 2011). Fourth, we can estimate $\delta^{15}N_{AA}$ values of trophic baseline in the

137 food web by offsetting trophic enrichment on the consumers. Despite the nitrogen in otolith organic tissue
138 is in the form of a proteinaceous matrix (Campana 1999) and seems to be originated from their diet
139 (Shiao et al. 2018), the analysis of $\delta^{15}N_{AA}$ is not applicable since the mass of organic components (only
140 about 3% of otolith mass: Campana 1999) are currently not enough to incremental analysis of $\delta^{15}N_{AA}$.
141 To clarify shifts in the population structure and/or TP associated with individual growth by
142 integrating isotopic tools, we focus on the Japanese flounder *Paralichthys olivaceus* in Sendai Bay, off the
143 Pacific coast of northern Japan (Fig. 1). *P. olivaceus* is abundant in benthic fish communities and is an
144 important species for commercial fisheries, stock enhancement, and aquaculture in temperate Japan
145 (Fisheries Agency and Fisheries Research and Education Agency of Japan 2019). Juveniles settle after the
146 planktonic stage at ca. 10 mm in total length and reach ca. 100 mm at the shallow sandy bottom (<0.5–3
147 m in depth) (Furuta et al. 1997a, 1997b, 1998, Kurita et al. 2018a). Their main food sources after settling
148 are mysids and small fish larvae (particularly the Japanese anchovy *Engraulis japonicus*) in shallow
149 nurseries and larger prey, such as shrimps, gobies, and bait fishes, in deeper habitats (20–100 m) (Yamada
150 et al. 1998; Tomiyama et al. 2013; Yamamoto and Tominaga 2014; Kurita et al. 2018a). However, the
151 main food sources for adults differ spatially, including *E. japonicus* in the northern area of the bay and the
152 Japanese sand lance *Ammodytes* spp. in the southern area of the bay (Togashi H., personal
153 communication). This difference can be explained by a difference in the sediment type (i.e., northern
154 silty-bottom area vs. southern sandy-bottom area; Gambe et al. 2014). In Sendai Bay, *P. olivaceus* has

155 been regarded as a single population based on a mitochondrial phylogeny (Shigenobu et al. 2013).
156 However, the habitat difference has only been established for adults, and migratory histories during
157 growth are still unclear. The role of behavioral groups within populations with divergent life
158 histories is also important for fisheries management and conservation (Kerr et al. 2010; Nims and
159 Walther 2014).

160 The purpose of this study was to clarify spatio-temporal variation on trophic role and
161 movements in *P. olivaceus* in Sendai Bay. Since *P. olivaceus* in Sendai Bay is regarded as the
162 member of single population (Yoneda et al. 2007b; Shigenobu et al. 2013; Kurita et al. 2018b), the
163 variation on these properties is directly related to the structural variation within a population, i. e.,
164 structure of sub-populations. To accomplish this goal, we 1) determined the relationship between
165 $\delta^{13}C_{bulk}$ and $\delta^{15}N_{bulk}$ values for the muscle and those for the outermost part of the vertebral centrum
166 to verify the ability to detect substances from recently consumed food, 2) analyzed $\delta^{13}C_{bulk}$ and
167 $\delta^{15}N_{bulk}$ values chronologically preserved in the vertebral centrum of individuals at different sites,
168 3) tracked shifts in trophic roles of individuals by a compound-specific stable isotope analysis of
169 nitrogen within amino acids, and 4) proposed an analytical approach to track individual-based
170 chronological movements for studies of the population dynamics of teleost fish species in
171 isoscapes. In our approach, comparison of time-series variation among the individuals can reveal
172 several components of population structure of *P. olivaceus* in Sendai Bay.

173

174 **Material and Methods**

175 **Study site and field sampling**

176 From June to July in 2016, adult *P. olivaceus* (age 3–5 years) were collected at four sampling sites in

177 Sendai Bay (Fig. 1), where residence time in summer was 18-21 and 39-44 days for fresh and brackish

178 water, respectively (Kakehi et al. 2012). Considering the spatial heterogeneity of Sendai Bay, two sites

179 with different depths were selected in the northern (N35 and N55: silty-bottom) and southern (S30 and

180 S45: sandy-bottom) areas (Gambe et al. 2014). Each number in the name of sampling site indicates

181 approximate water depth (m) of the site. Individuals were collected by bottom trawling (mesh size: 5 mm)

182 using the *Wakataka Maru*, a 692-ton research vessel belonging to the Tohoku National Fisheries Research

183 Institute, or smaller trawling boats (9.7 tons). A ship speed of 2.5–3.0 knots was maintained during

184 sampling, and bottom trawling was carried out for 30 min. Otoliths were collected individually and stored

185 in a freezer until dissection in the laboratory. Sampled otoliths were dried naturally in the laboratory and

186 stored until analysis.

187

188 **Preparation of bone collagen and muscle samples**

189 Muscle tissues were immersed in a methanol–chloroform mixture (1:1, vol:vol) for 12 h for defatting. The

190 samples were rinsed at least twice with 99.5% methanol until the resolved fat was completely removed.

191 Then, samples were freeze-dried, powdered, and stored until analysis. Bone collagen samples were
192 prepared following the method described by Matsubayashi et al. (2017). The veretebral centrums were
193 immersed in a methanol:chloroform mixture (1:1, vol:vol) for approximately 6 h and were rinsed twice
194 with 99.5% methanol. The remaining solvent was allowed to completely evaporate at ambient
195 temperature. Then, the vertebral centrums were well-shaped by microgrinder. Next, the samples were
196 immersed in 0.1 M NaOH, and then 1.0 M HCl both for about 12 h. After each treatment, samples were
197 rinsed twice with Milli-Q water, respectively. Finally, samples were heated in Milli-Q water at 90°C for
198 about 12 h and then freeze-dried. Comparing with the method by Matsubayashi et al. (2017), we made
199 following modifications. 1) In addition to a micro-grinder, an ultrasonic scaler (Varios 970, NSK) was
200 used to remove the spongy bone around the notochordal pore of the vertebral centrum (Fig. 2) where the
201 vertebral centrum is thinner than the outer part, to decrease over-scraping. 2) The length of each vertebral
202 centrum was measured to the nearest 1 μm using a digital micrometer, and the thickness of the section
203 comparable to growth over 2 months was estimated using following equation:
204
205 $$T_{2month} = \left(H_{centrum} \times L_{age3}\right)/(L_{whole} \times 18),$$
206
207 where $T_{2\mathrm{month}}$, H_{centrum}, L_{age3}, and L_{whole} represent the thickness of the section corresponding to growth in 2
208 months, total height of the target centrum, length from the apex to the third translucent band, and length

209 from the apex to the outermost edge of the centrum, respectively (Fig. 2). To measure L_{age3} and L_{whole}, a
210 partially modified burn method (Fujinami et al. 2018) was used to clarify growth bands by sagittally
211 cutting the 10th or 11th abdominal vertebra. Age and growth bands were cross-checked by observing the
212 otolith of same individual. 3) In this study, 12th or later vertebrae were used because the shapes of the
213 vertebral centrum in dorsal vertebra (i.e., prior to the 12th) are distorted and far from concentric in this
214 Heterosomata fish (Kato et al., personal observation). 4) Each vertebral centrum was subdivided into
215 sections with a thickness of T_{2month}, from the apex to the edge, using a sliding microtome (REM-710
216 Retratom; Yamato Kohki Industrial, Tokyo, Japan) under frozen conditions with Milli-Q water at −20°C
217 using a refrigeration unit (MC-802A Electro Freeze; Yamato Kohki Industrial). 5) According to Van
218 Klinken (1999), a collagen C/N ratio in the range of 2.9–3.5 was regarded as pure. Despite Guiry and
219 Szpak (2020) recently established narrower criterion (3.00–3.30 for modern tissues of fish), we applied
220 wider range since appropriate criterion for the juvenile period is still unclear.
221
222 **Stable isotope analyses**
223 Carbon and nitrogen stable isotope ratios for all individuals were measured in both bone collagen and
224 muscle samples using a mass spectrometer (Delta XP; Thermo Fisher Scientific, Waltham, MA)
225 connected to an elemental analyzer (Flash EA 1112; Thermo Fisher Scientific) via an interface (Conflo
226 III; Thermo Fisher Scientific). The stable isotope ratios are expressed in δ notation as deviations from a

227 standard: $\delta^{13}C$ or $\delta^{15}N = R_{sample}/R_{standard} - 1$, where R is $^{13}C/^{12}C$ for $\delta^{13}C$ and $^{15}N/^{14}N$ for $\delta^{15}N$. The $R_{standard}$

228 values for carbon and nitrogen were those of Vienna Pee Dee Belemnite and atmospheric N_2, respectively.

229 Data were corrected using multiple internal standards (CERKU-01 and CERKU-02) calibrated with

230 international standards (Tayasu et al. 2011). 8 to 10 samples were run between each standard. Analytical

231 errors (1σ) of the standards in the $\delta^{13}C$ and $\delta^{15}N$ measurements were within 0.04‰ and 0.12‰,

232 respectively.

233 Samples for $\delta^{15}N_{AA}$ measurements were prepared following the method of Ishikawa et al.

234 (2014). Amino acids in all samples were purified for a compound-specific isotope analysis by HCl

235 hydrolysis, followed by the addition of *N*-pivaloyl/isopropyl (Pv/iPr). In brief, about 3 mg of each

236 sample material was hydrolyzed with 12 N HCl at 110°C for 12 h. The hydrolysate was washed

237 with *n*-hexane/dichloromethane (3:2, v/v) to remove hydrophobic constituents, such as lipids, and

238 then evaporated to dryness under an N_2 stream. After derivatization with thionyl chloride/2-

239 propanol (1:4, v/v) at 110°C for 2 h and with pivaloyl chloride/dichloromethane (1:4, v/v) at 110°C

240 for 2 h, the Pv/iPr derivatives of amino acids were extracted with dichloromethane. $\delta^{15}N_{AA}$ was

241 measured following the method of Chikaraishi et al. (2010b), with modifications. Briefly, the $\delta^{15}N$

242 values for individual amino acids were determined by gas chromatography/combustion/isotope

243 ratio mass spectrometry (GC/C/IRMS) using the Thermo Delta V Advantage (Thermo Fisher

244 Scientific) coupled to a gas chromatograph (Trace GC ULTRA; Thermo Fisher Scientific) via a

245 modified GC-Isolink interface consisting of combustion and reduction furnaces and the Conflo IV
246 interface (Thermo Fisher Scientific). Combustion was performed in a microvolume ceramic tube with
247 CuO, NiO, and Pt wires at 1030°C, and reduction was performed in a microvolume ceramic tube with a
248 reduced Cu wire at 650°C. The GC was equipped with an Ultra-2 capillary column (50m, 0.32 mm
249 i.d.,0.52 mm film thickness; Agilent Technologies, Santa Clara, CA). The GC oven temperature was
250 programmed as follows: initial temperature of 40°C for 2.5 min, ramp up at 15°C min^{-1} to 110°C, ramp
251 up at 3°C min^{-1} to 150°C, ramp up at 6°C min^{-1} to 220°C, and dwell for 14 min. Carrier gas (He) flow
252 through the GC column was 1.4 ml min^{-1}. The CO_2 generated in the combustion furnace was eliminated
253 by a liquid nitrogen trap. Standard mixtures of 5–15 amino acids with known $\delta^{15}N$ were analyzed every
254 1–6 samples to confirm the reproducibility of the isotope measurements. Analytical errors (1σ) of the
255 standards were better than 0.8‰, with a minimum sample amount of 60 ng N.
256
257 **Data analysis**
258 Pearson's correlation analysis was used to compare the $\delta^{13}C_{bulk}$ and $\delta^{15}N_{bulk}$ values of collagen in the
259 outermost edge of the vertebral centrum with those of muscle tissues from the same individual. A
260 nonlinear Laplacian spectral analysis (Giannakis and Majda 2012: nonlinear time-series analysis
261 hereafter: see Supplementary text S1 for method details) was used to uncover salient modes of variability
262 from chronological isotopic information with measurement noise and timing uncertainty. This analysis

allows us to detect nonlinear variability of complex dynamics by employing a Laplacian eigenmap (Coifman and Lafon 2006). The $\delta^{13}C_{bulk}$ and $\delta^{15}N_{bulk}$ values were analyzed simultaneously in vertebral section numbers 2–18, where missing values did not exist, with a few exceptions, and modes of variability were extracted if the proportion of explained variance was larger than the average. The tuning parameters of nonlinear Laplacian spectral analysis were determined to extract yearly variability of *P. olivaceus* population dynamics (Supplementary text S1). The robustness of our results was confirmed by sensitivity analysis (Supplementary text S2 & Supplementary Fig. S1). Prior to the nonlinear time-series analysis, a few missing values were interpolated with the mean value at the nearest-neighbor sections, and all values were standardized (mean 0 and variance 1) for each element.

To detect changes in structural components in the population during growth, $\delta^{13}C_{bulk}$ and $\delta^{15}N_{bulk}$ values were compared among the four sampling sites by an analysis of variance for each section of the vertebral centrum. Bonferroni tests were used for *post hoc* comparisons.

Furthermore, we tracked TPs calculated from the incremental bone collagen dataset. In most previous studies, possible trophic sources in focused food webs were either aquatic primary producers or terrestrial C3 plants. In such cases, the TP of consumers was calculated by the following equation:

$$\mathrm{TP} = (\delta^{15}\mathrm{N}_{\mathrm{Glu}} - \delta^{15}\mathrm{N}_{\mathrm{Phe}} + \beta_{\mathrm{Glu/Phe}})/7.6 + 1,$$

where $\delta^{15}N_{Glu}$ and $\delta^{15}N_{Phe}$ are nitrogen isotopic compositions of glutamic acid and phenylalanine, respectively. $\beta_{Glu/Phe}$ represents the difference between $\delta^{15}N$ values of glutamic acid and phenylalanine in primary producers (−3.4‰ for aquatic primary producers and +8.4‰ for terrestrial C3 plants: Chikaraishi et al. 2009, 2011). We assumed that aquatic primary producers are dominant trophic source through the life cycle of *P. olivaceus* and adopted −3.4‰ as the constant number for the formula. Furthermore, we defined the trophic baseline ($\delta^{15}N_{Base}$) as the $\delta^{15}N_{Phe}$ of primary trophic sources, i.e., primary producers consumed by the fishes directly or indirectly, and calculated it by following equation:

$$\delta^{15}\mathrm{N}_{\mathrm{Base}} = \delta^{15}\mathrm{N}_{\mathrm{Phe}} - 0.4 \times (\mathrm{TP} - 1).$$

R version 3.6.3 (R Core Team 2020) was used for statistical analysis. Despite health status such as starvation can also affect $\delta^{13}C$ and $\delta^{15}N$ of consumers (Gorokhova 2018; Karlson et al. 2018), we didn't consider the factor since chronological changes of physical condition is unclear in our samples.

Results

In total, we caught and processed 19 individuals of *P. olivaceus* at four sampling sites for $\delta^{13}C_{bulk}$ and $\delta^{15}N_{bulk}$ measurement of bulk vertebral collagen (Fig. 1, Supplementary Tables S1–S3). For most samples, the C/N molar ratio fell within the quality criterion (Table S4). The minimum, maximum, and mean total

299 length values were 447 mm, 654 mm, and 544 ± 59 mm (mean ± 1σ), respectively. $\delta^{13}C_{bulk}$ and $\delta^{15}N_{bulk}$

300 values for collagen in the outermost edge of the vertebral centrum were correlated with those of muscle

301 tissues from the same individual ($r^2 = 0.52$, $p < 0.05$ for $\delta^{13}C_{bulk}$; $r^2 = 0.54$, $p < 0.05$ for $\delta^{15}N_{bulk}$; Fig. 3).

302 In a nonlinear time-series analysis, we extracted four major modes of variability (explaining

303 32.8%, 16.0%, 11.2%, and 9.3% of the variance, respectively; Supplementary Fig. S2). Each mode

304 represented a different type of chronological isotopic information (Fig. 4). In the first mode (Figs.

305 4a, e and 5), isotopic variation among individuals was larger than that within individuals. In

306 particular, $\delta^{15}N_{bulk}$ values showed large inter-individual variation compared with that of $\delta^{13}C_{bulk}$

307 values. We found obvious isotopic separation between N55 and other sampling sites; individuals at

308 N55 had obviously lower $\delta^{15}N_{bulk}$ values than those of individuals at other sampling sites. The

309 phases were unsynchronized among individuals in the second mode, and all individuals showed up

310 to one period during their lifetime (Fig. 4b, f). In the third mode, there was greater variation among

311 individuals at younger ages (i.e., until about 1.5 years) than in subsequent adult periods (Fig. 4c, g).

312 In the fourth mode, quite clear patterns with a period of approximately six vertebral sections were

313 detected in both $\delta^{13}C_{bulk}$ and $\delta^{15}N_{bulk}$ values (Fig. 4d, h).

314 Among the four sampling sites, $\delta^{13}C_{bulk}$ values for vertebral collagen at sections 1–15, 17,

315 and 18 did not show significant differences (Table 1a, Fig. 6a). $\delta^{13}C_{bulk}$ values commonly increased

316 from the 1st to the 4th or 5th section and then remained nearly constant or decreased slightly but

317 continuously toward the outermost vertebral section at all sampling sites (Fig. 6a). In contrast, site-
318 specific differences during growth were observed in $\delta^{15}N_{bulk}$ values for vertebral collagen (Table 1b, Fig.
319 6b). The $\delta^{15}N_{bulk}$ values for individuals collected at N55 were significantly lower than those at the
320 remaining three sites at sections 1–9 and 12. Then the $\delta^{15}N_{bulk}$ values for individuals collected at N35 and
321 S45 decreased to the levels observed in individuals collected at N55, and the differences were not
322 significant in sections later than 13 (except sections 10 and 11 at S45). Only individuals collected at S30
323 showed significantly higher $\delta^{15}N_{bulk}$ values than those of individuals at N55 throughout all sections.
324 We measured $\delta^{15}N_{Glu}$ and $\delta^{15}N_{Phe}$ in 32 vertebral collagen samples from 11 individuals
325 (Supplementary Tables S5, S6). TPs of *P. olivaceus* mostly increased during growth in the range of 1.7 to
326 3.1 (Fig. 7a, Supplementary Table S7). In general, $\delta^{15}N_{Base}$ values for *P. olivaceus* decreased with growth
327 in the range of 8.1‰ to 3.9‰ (Fig. 7b, Supplementary Table S8).
328
329 **Discussion**
330 The significant correlations in both $\delta^{13}C_{bulk}$ or $\delta^{15}N_{bulk}$ values between muscle and vertebral collagen at
331 the outermost edge of the vertebral centrum suggest that collagen of vertebral centrum at the arbitrary
332 time could reflect the values of the muscle at the same time when the vertebral centrum section was
333 formed in trophic analysis. However, the trends were offset from a 1:1 line both in $\delta^{13}C_{bulk}$ or $\delta^{15}N_{bulk}$
334 (Fig. 3). Therefore, we should consider the differences in the dynamics of ^{13}C and ^{15}N when these tissues

335 are produced and metabolized. Moreover, further validation, such as analysis of trophic discrimination
336 factors in bone collagen (Matsubayashi et al. 2019), must be conducted to determine the origin and/or
337 migration history of various fishes at the individual level.

338 We detected individual-based variation in $\delta^{13}C_{bulk}$ and $\delta^{15}N_{bulk}$ values in *P. olivaceus* in
339 Sendai Bay. The results of a nonlinear time-series analysis suggested that a combination of intrinsic
340 and extrinsic factors determine the isotopic chronology obtained from a segmental analysis of
341 vertebral collagen. The first mode (Figs. 4a, e and 5) reflects the lifetime difference in $\delta^{15}N_{bulk}$
342 values among sampling sites, with distinctly lower $\delta^{15}N_{bulk}$ values for individuals at N55. It also
343 suggests that habitat and/or food sources experienced by individuals from N55 were not identical to
344 those of individuals collected at the other three sites. Isotopic variation within an individual during
345 growth is explained by the second mode (Fig. 4b, f). Relatively greater isotopic variation and
346 higher amplitudes in younger periods in the third mode (Fig. 4c, g) reflect individual differences in
347 the timing of migration from the nursery to deep offshore areas in juvenile *P. olivaceus* in Sendai
348 Bay (Kurita et al. 2018a). The fourth mode showed approximate annual cycles (Fig. 4d, h),
349 suggesting that factors related to seasonality, such as changes in food availability and reproductive
350 behavior, are also recorded in the isotopic chronology obtained from vertebral collagen. Since the
351 majority of *P. olivaceus* matures sexually at two years of age in Sendai Bay (Yoneda et al. 2007a),
352 the first annual cycles shown in Fig 4d and 4h must not be related to reproductive behavior. One of

353 potential reasons of such annual dynamics is seasonal migration of *P. olivaceus*. Biologging data revealed
354 that *P. olivaceus* around Fukushima Prefecture generally migrates to shallower area in summer and
355 migrate back to deeper area in winter (Kurita et al. accepted). Since the sea area is neighboring and shows
356 similar physical property with Sendai Bay, same seasonal pattern of migration in *P. olivaceus* is strongly
357 suggested in Sendai Bay. To clarify the factors affecting variation among individuals, both the isotope
358 ratios of food items (mainly mysids and small fish larvae for juveniles and larger prey, such as shrimps,
359 gobies, and bait fishes, for adults: Yamada et al. 1998, Tomiyama et al. 2013, Yamamoto et al. 2014,
360 Kurita et al. 2018a) and $\delta^{15}N_{Base}$ values incorporating the dynamics of seawater and freshwater inputs
361 from coastal land areas are required. For this purpose, detailed isoscapes of $\delta^{13}C_{bulk}$ and $\delta^{15}N_{bulk}$ values in
362 Sendai Bay and surrounding areas need to be developed both in vertically and horizontall**y**. Generally,
363 heterogeneity in $\delta^{13}C_{bulk}$ and $\delta^{15}N_{bulk}$ values in ocean isoscapes is considered to be caused by productivity
364 dynamics, ocean currents and upwelling, and the degree of atmospheric fixation of carbon and nitrogen
365 (Kurle and McWhorter 2017, Sogawa et al. 2017). Latitudinal variation in $\delta^{13}C$ values in phytoplankton is
366 caused by a kinetic isotope effect associated with geographical variation in biosynthesis and metabolism
367 (Rau et al. 1982, Goericke and Fry 1994). Wada et al. (2012) also suggested that $\delta^{15}N_{bulk}$ values for
368 plankton are closely correlated with the chemical forms of inorganic nitrogen used by primary producers.
369 Therefore, isotopic signatures of *P. olivaceus* likely reflect the averaged variation over large spatial scales
370 (e.g., ocean area).

371 Among the four sampling sites, $\delta^{15}N_{bulk}$ values for the vertebral collagen of sections 1–9 and
372 11 were lowest for individuals collected at N55 (Fig. 6). These results suggest that the habitat
373 and/or food sources at this site differed from those of the other three sites. Two hypotheses may
374 explain this pattern: 1) individuals at each site did not move substantially during their lifetimes or
375 2) individuals migrated synchronically. In particular, $\delta^{15}N_{bulk}$ values for vertebral collagen showed
376 consistently significant differences between individuals at S30 and N55 (Fig. 6). These results
377 suggest that the habitat and/or food sources did not overlap throughout their lifetimes until catch.
378 Considering that the observed variation in $\delta^{15}N_{bulk}$ values of vertebral collagen was greater among
379 sites than among individuals, these results strongly suggest that there were at least two groups of *P.*
380 *olivaceus* during the early migration history in Sendai Bay. Furthermore, these results also indicate
381 a variety in nursery environment of *P. olivaceus* in the coast of Sendai Bay. Since biotic and abiotic
382 environments in the shallow habitat < 15 m in depth are appropriate as nursery grounds for *P.*
383 *olivaceus* in Sendai Bay (Kurita et al. 2018a), a wide extent of the shore is regarded as suitable
384 habitat for juveniles. Therefore, it is the next challenge to clarify the environmental heterogeneity
385 in Sendai Bay and to predict the nursery areas of every adults.
386 Drastic increases in $\delta^{13}C_{bulk}$ values of vertebral collagen in the juvenile period (i.e., sections
387 1–4) at all four sampling sites (Fig. 6) offer the potential to determine the timing of migration from
388 the nursery to deep offshore habitats in juvenile *P. olivaceus*. Given that the timing varies over 10

389 months (from November to the following September) among age-0 juvenile individuals in Sendai Bay
390 (Kurita et al. 2018a), it is possible to reveal the relationship between migration timing and later growth by
391 applying our approach. The fourth mode of variation in the nonlinear time-series analysis showed
392 approximate annual cycles (Fig. 4d, h), and sections 1–8 seem to reflect age-0 juveniles. Therefore,
393 rigorous matching of the thickness of each section in the vertebral centrum with an accurate time scale is
394 needed for a detailed time series analysis (Togashi H., in preparation).
395 Analyses of $\delta^{15}N_{Glu}$ and $\delta^{15}N_{Phe}$ of vertebral collagen revealed that TPs increased for each
396 individual (Fig. 7a). This can be explained by an ontogenetic shift in food items (i.e., mainly mysids and
397 small fish larvae for juveniles and larger prey including shrimps, gobies, and bait fishes, such as Japanese
398 anchovy, for adults: Yamada et al. 1998, Tomiyama et al. 2013, Yamamoto et al. 2014, Kurita et al.
399 2018a). However, the estimated TPs were generally lower than those expected from their food items (i.e.,
400 >3 for juveniles and >4 for adults). TPs have similarly been underestimated for *P. olivaceus* in Tokyo Bay,
401 Japan (Kobayashi et al. 2019) and the ridged-eye flounder *Pleuronichthys cornutus* in Masan Bay, South
402 Korea (Won et al. 2020). This common underestimation in Pleuronectiformes in compound-specific
403 isotope analysis of amino acids needs to be resolved. We also detected a decrease in $\delta^{15}N_{Base}$ values for
404 most individuals (Fig. 7b). Gambe et al. (2014) suggested that the contribution from terrestrial organic
405 matter is relatively high in the shallow southern coastal parts of Sendai Bay. Furthermore, areas
406 downstream of inflowing rivers to Sendai Bay are dominated by paddy fields and urban areas, where

407 human-induced nitrogen discharge with high $\delta^{15}N$ values occurs. In contrast, active water exchange
408 in Sendai Bay (Kakehi et al. 2012) suggests that the effects of high $\delta^{15}N$ values from terrestrial
409 areas are limited around coastal areas. Considering movement along with growth, the decrease in
410 $\delta^{15}N_{Base}$ values in *P. olivaceus* (Fig. 7b) may reflect baseline differences between shallow nursery
411 habitats and deeper adult habitats. Since it is difficult to estimate isotopic transitions along the
412 individual growth using muscle tissues, our use of segmental isotope analysis of vertebral collagen
413 has an advantage with respect to clarifying shifts of population structure and/or trophic roles
414 associated with individual growth in teleost fishes.

415 Spatial structure within fish populations can affect overall dynamics because habitat
416 differences can impact abundance, growth, reproduction, maturity, recruitment, and survival
417 (Hayes et al. 1996). For example, resident and migratory groups can exist within the same genetic
418 population, termed “partial migration” (Kerr et al. 2009). Our results suggest that most adult *P.*
419 *olivaceus* individuals at N55 belong to a migratory contingent (i.e., they are clearly distinguishable)
420 within the population throughout their life history in Sendai Bay. In particular, our chronological
421 approach effectively clarifies the spatio-temporal dynamics of contingent structures within the
422 population. Furthermore, our detailed individual-based approach can be used for the *post hoc*
423 detection of various processes, such as migration, habitat selection, and trophic shifts (Wilson
424 1998; Conrad et al. 2011). Combining the information obtained from traditional population

research and isotopic features of tissues other than the vertebral centrum (e.g., otoliths) and other elements (e.g., $\delta^{18}O$), we can reconstruct more detailed structures within populations of teleost fishes.

References

Ankjærø T, Christensen JT, Grønkjær P (2012) Tissue-specific turnover rates and trophic enrichment of stable N and C isotopes in juvenile Atlantic cod *Gadus morhua* fed three different diets. Mar Ecol Prog Ser 461:197–209. doi: 10.3354/meps09871

Bowen GJ (2010) Isoscapes: Spatial Pattern in Isotopic Biogeochemistry. Annu Rev Earth Planet Sci 38:161–187. doi: 10.1146/annurev-earth-040809-152429

Bradbury IR, DiBacco C, Thorrold SR, Snelgrove PVR, Campana SE (2011) Resolving natal tags using otolith geochemistry in an estuarine fish, rainbow smelt *Osmerus mordax*. Mar Ecol Prog Ser 433:195–204. doi: 10.3354/meps09178

Brownscombe JW, Lédée EJI, Raby GD, Struthers DP, Gutowsky LFG, Nguyen VM, Young N, Stokesbury MJW, Holbrook CM, Brenden TO, Vandergoot CS, Murchie KJ, Whoriskey K, Mills Flemming J, Kessel ST, Krueger CC, Cooke SJ (2019) Conducting and interpreting fish telemetry studies: considerations for researchers and resource managers. Rev Fish Biol Fish 29:369–400. doi: 10.1007/s11160-019-09560-4

Campana SE (1999) Chemistry and composition of fish otoliths: Pathways, mechanisms and applications.

443 Mar Ecol Prog Ser 188:263–297. doi: 10.3354/meps188263

444 Chikaraishi Y, Ogawa NO, Kashiyama Y, Takano Y, Suga H, Tomitani A, Miyashita H, Kitazato H,

445 Ohkouchi N (2009) Determination of aquatic food-web structure based on compound-specific

446 nitrogen isotopic composition of amino acids. Limnol Oceanogr Methods 7:740–750. doi:

447 10.4319/lom.2009.7.740

448 Chikaraishi Y, Ogawa NO, Takano Y, Tsuchiya M, Ohkouchi N (2010) Food chain analysis by nitrogen

449 isotopic composition of amino acids. Chikyukagaku 44:233–241 (in Japanese with English abstract)

450 Chikaraishi Y, Ogawa NO, Doi H, Ohkouchi N (2011) $^{15}N/^{14}N$ ratios of amino acids as a tool for studying

451 terrestrial food webs: A case study of terrestrial insects (bees, wasps, and hornets). Ecol Res

452 26:835–844. doi: 10.1007/s11284-011-0844-1

453 Coifman RR, Lafon S (2006) Diffusion maps. Appl Comput Harmon Anal 21:5–30. doi:

454 10.1016/j.acha.2006.04.006

455 Conrad JL, Weinersmith KL, Brodin T, Saltz JB, Sih A (2011) Behavioural syndromes in fishes: A

456 review with implications for ecology and fisheries management. J Fish Biol 78:395–435. doi:

457 10.1111/j.1095-8649.2010.02874.x

458 Cook BD, Bunn SE, Hughes JM (2007) Molecular genetic and stable isotope signatures reveal

459 complementary patterns of population connectivity in the regionally vulnerable southern pygmy

460 perch (*Nannoperca australis*). Biol Conserv 138:60–72. doi: 10.1016/j.biocon.2007.04.002

461 Cooke SJ, Woodley CM, Eppard MB, Brown RS, Nielsen JL (2011) Advancing the surgical implantation
462 of electronic tags in fish: A gap analysis and research agenda based on a review of trends in
463 intracoelomic tagging effects studies. Rev Fish Biol Fish 21:127–151. doi: 10.1007/s11160-010-
464 9193-3
465 Cowen RK, Paris CB, Srinivasan A (2006) Scaling of connectivity in marine populations. Science
466 311:522–527. doi: 10.1126/science.1122039
467 DeNiro MJ, Epstein S (1978) Influence of diet on the distribution of carbon isotopes in animals. Geochim
468 Cosmochim Acta 42:495–506. doi: 10.1002/mop.25285
469 DeNiro MJ, Epstein S (1981) Influence of diet on the distribution of nitrogen isotopes in animals.
470 Geochim Cosmochim Acta 45:341–351.
471 Doubleday ZA, Cliff J, Izzo C, Gillanders BM (2018) Untapping the potential of sulfur isotope analysis
472 in biominerals. Mar Ecol Prog Ser 598:159–166. doi: 10.3354/meps12605
473 Estrada JA, Rice AN, Natanson LJ, Skomal GB (2016) Use of isotopic analysis of vertebrae in
474 reconstructing ontogenetic feeding ecology in white sharks. Ecology 87:829–834.
475 Fisheries Agency and Fisheries Research and Education Agency of Japan (2019) Marine fisheries stock
476 assessment and evaluation for Japanese waters (fiscal year 2018/2019).
477 Fraile I, Arrizabalaga H, Santiago J, Goñi N, Arregi I, Madinabeitia S, David Wells RJ, Rooker JR (2016)
478 Otolith chemistry as an indicator of movements of albacore (*Thunnus alalunga*) in the North

Atlantic Ocean. Mar Freshw Res 67:1002–1013. doi: 10.1071/MF15097

Fujinami Y, Semba Y, Ohshimo S, Tanaka S (2018) Development of an alternative ageing technique for blue shark (*Prionace glauca*) using the vertebra. J Appl Ichthyol 34:590–600. doi: 10.1111/jai.13620

Furuta S, Watanabe T, Yamada H, Nishida T, Miyanaga T (1997a) Changes in distribution, growth and abundance of hatchery-reared Japanese flounder *Paralichthys olivaceus* released in the coastal area of Tottori Prefecture. Nippon Suisan Gakkaishi 63:877–885 (in Japanese with English abstract)

Furuta S, Watanabe T, Yamada H, Miyanaga T (1997b) Changes in feeding condition of released hatchery-reared Japanese flounder, *Paralichthys olivaceus*, and prey mysid density in the coastal area of Tottori prefecture. Nippon Suisan Gakkaishi 63:886–891 (in Japanese with English abstract)

Furuta S, Watanabe T, Yamada H (1998) Predation by fishes on hatchery-reared Japanese flounder *Paralichthys olivaceus* juveniles released in the coastal area of Tottori Prefecture. Nippon Suisan Gakkaishi 64:1–7 (in Japanese with English abstract)

Gambe S, Oota H, Suzuki N, Ito K, Sasaki K, Inomata K, Nakagawa R (2014) Presumption of sediment movement in Sendai Bay caused by Pacific coast of Tohoku earthquake tsunami, according to comparison of C, N quantity and stable isotope ratio. Miyagi Prefect Rep Fish Sci 14:1–10 (in Japanese)

Gao Y, Bean D (2008) Stable isotope analyses of otoliths in identification of hatchery origin of Atlantic

497 salmon (*Salmo salar*) in Maine. Environ Biol Fishes 83:429–437. doi: 10.1007/s10641-008-9365-3

498 Gaston TF, Suthers IM (2004) Spatial variation in δ^{13}C and δ^{15}N of liver, muscle and bone in a rocky reef

499 planktivorous fish: The relative contribution of sewage. J Exp Mar Bio Ecol 304:17–33. doi:

500 10.1016/j.jembe.2003.11.022

501 Giannakis D, Majda AJ (2012) Nonlinear Laplacian spectral analysis for time series with intermittency

502 and low-frequency variability. Proc Natl Acad Sci U S A 109:2222–2227. doi:

503 10.1073/pnas.1118984109

504 Goericke R, Fry B (1994) Variations of marine plankton δ^{13}C with latitude, temperature, and dissolved

505 CO_2 in the world ocean. Grobal Biogeochem Cycles 8:85–90.

506 Gorokhova E (2018) Individual growth as a non-dietary determinant of the isotopic niche metrics.

507 Methods Ecol Evol 9:269–277. doi: 10.1111/2041-210X.12887

508 Green BC, Smith DJ, Grey J, Underwood GJC (2012) High site fidelity and low site connectivity in

509 temperate salt marsh fish populations: a stable isotope approach. Oecologia 168:245–255. doi:

510 10.1007/S00442-01

511 Grønkjær P, Pedersen JB, Ankjærø TT, Kjeldsen H, Heinemeier J, Steingrund P, Nielsen JM, Christensen

512 JT (2013) Stable N and C isotopes in the organic matrix of fish otoliths: Validation of a new

513 approach for studying spatial and temporal changes in the trophic structure of aquatic ecosystems.

514 Can J Fish Aquat Sci 70(2), 143-146 70:143–146.

515 Guiry EJ, Szpak P (2020) Quality control for modern bone collagen stable carbon and nitrogen isotope
516 measurements. Methods Ecol Evol 11:1049–1060. doi: 10.1111/2041-210X.13433
517 Hayes DB, Ferreri CP, Taylor WW (1996) Linking fish habitat to their population dynamics. Can J Fish
518 Aquat Sci 53:383–390. doi: 10.1139/f95-273
519 Hobson KA, Clark RG (1992) Assessing Avian Diets Using Stable Isotopes I: Turnover of ^{13}C in Tissues.
520 Condor 94:181–188. doi: 10.2307/1368807
521 Ishikawa NF, Kato Y, Togashi H, Yoshimura M, Yoshimizu C, Okuda N, Tayasu I (2014) Stable nitrogen
522 isotopic composition of amino acids reveals food web structure in stream ecosystems. Oecologia
523 175:911–922. doi: 10.1007/s00442-014-2936-4
524 Kaifu K, Itakura H, Amano Y, Shirai K, Yokouchi K, Wakiya R, Murakami-Sugihara N, Washitani I,
525 Yada T (2018) Discrimination of wild and cultured Japanese eels based on otolith stable isotope
526 ratios. ICES J Mar Sci 75:719–726. doi: 10.1093/icesjms/fsx173
527 Kakehi S, Ito S, Yagi H, Wagawa T (2012) Estimation of the residence time of fresh and brackish water
528 in Sendai Bay. J Japan Soc Civ Eng Ser B2 (Coastal Eng) 68:I_951–I_955. doi:
529 10.2208/kaigan.68.i_951 (in Japanese with English abstract)
530 Karlson AML, Reutgard M, Garbaras A, Gorokhova E (2018) Isotopic niche reflects stress-induced
531 variability in physiological status. R Soc Open Sci. doi: 10.1098/rsos.171398
532 Kerr LA, Andrews AH, Cailliet GM, Brown TA, Coale KH (2006) Investigations of $\Delta^{14}C$, $\delta^{13}C$, and $\delta^{15}N$

533 in vertebrae of white shark (*Carcharodon carcharias*) from the eastern North Pacific Ocean.
534 Environ Biol Fishes 77:337–353. doi: 10.1007/s10641-006-9125-1
535 Kerr LA, Secor DH, Piccoli PM (2009) Partial migration of fishes as exemplified by the estuarine-
536 dependent white perch. Fisheries 34:114–123. doi: 10.1577/1548-8446-34.3.114
537 Kerr LA, Cadrin SX, Secor DH (2010) The role of spatial dynamics in the stability, resilience, and
538 productivity of an estuarine fish population. Ecol Appl 20:497–507. doi: 10.1890/08-1382.1
539 Kobayashi J, Yoshimoto M, Yamada K, Okamura K, Sakurai T (2019) Comparison of trophic
540 magnification factors of PCBs and PBDEs in Tokyo Bay based on nitrogen isotope ratios in bulk
541 nitrogen and amino acids. Chemosphere 226:220–228. doi: 10.1016/j.chemosphere.2019.03.133
542 Kurita Y, Okazaki Y, Yamashita Y (2018a) Ontogenetic habitat shift of age-0 Japanese flounder
543 *Paralichthys olivaceus* on the Pacific coast of northeastern Japan: differences in timing of the shift
544 among areas and potential effects on recruitment success. Fish Sci 84:173–187. doi:
545 10.1007/s12562-018-1180-y
546 Kurita Y, Togashi H, Hattori T, Shibata Y (2018b) Stock assessment and evaluation for the Japanese
547 flounder stock in the Pacific coast of northern Japan in fiscal year 2017. In: Japan Fisheries
548 Research and Education Agency (ed) Marine fisheries stock assessment and evaluation for Japanese
549 waters (fiscal year 2017). Tokyo,
550 Kurita Y, Sakuma T, Kakehi S, Shimamura S, Sanematsu A, Kitagawa H, Ito S, Kawabe R, Shibata Y,

551 Tomiyama T. (accepted) Seasonal changes in depth and temperature of habitat for Japanese flounder
552 *Paralichthys olivaceus* on the Pacific coast of northeastern Japan. Fish Sci doi: 10.1007/s12562-021-
553 01495-9
554 Kurle CM, McWhorter JK (2017) Spatial and temporal variability within marine isoscapes: Implications
555 for interpreting stable isotope data from marine systems. Mar Ecol Prog Ser 568:31–45. doi:
556 10.3354/meps12045
557 Maberly SC, Raven JA, Johnston AM (1992) Discrimination between ^{12}C and ^{13}C by marine plants.
558 Oecologia 91:481–492. doi: 10.1007/BF00650320
559 Matsubayashi J, Saitoh Y, Osada Y, Uehara Y, Habu J, Sasaki T, Tayasu I (2017) Incremental analysis of
560 vertebral centra can reconstruct the stable isotope chronology of teleost fishes. Methods Ecol Evol
561 8:1755–1763. doi: 10.1111/2041-210X.12834
562 Matsubayashi J, Umezawa Y, Matsuyama M, Kawabe R, Mei W, Wan X, Shimomae A, Tayasu I (2019)
563 Using segmental isotope analysis of teleost fish vertebrae to estimate trophic discrimination factors
564 of bone collagen. Limnol Oceanogr Methods 17:87–96. doi: 10.1002/lom3.10298
565 Matsubayashi J, Osada Y, Tadokoro K, Abe Y, Yamaguchi A, Shirai K, Honda K, Yoshikawa C, Ogawa
566 NO, Ohkouchi N, Ishikawa NF, Nagata T, Miyamoto H, Nishino S, Tayasu I (2020) Tracking long-
567 distance migration of marine fishes using compound-specific stable isotope analysis of amino acids.
568 Ecol Lett 1–10. doi: 10.1111/ele.13496
569 Mellon-Duval C, De Pontual H, Métral L, Quemener L (2010) Growth of European hake (*Merluccius*

570 *merluccius*) in the Gulf of Lions based on conventional tagging. ICES J Mar Sci 67:62–70. doi:
571 10.1093/icesjms/fsp215
572 Moore JW, Semmens BX (2008) Incorporating uncertainty and prior information into stable isotope
573 mixing models. Ecol Lett 11:470–480. doi: 10.1111/j.1461-0248.2008.01163.x
574 Nims MK, Walther BD (2014) Contingents of Southern Flounder from subtropical estuaries revealed by
575 otolith chemistry. Trans Am Fish Soc 143:721–731. doi: 10.1080/00028487.2014.892535
576 Ohkouchi N, Chikaraishi Y, Close HG, Fry B, Larsen T, Madigan DJ, McCarthy MD, McMahon KW,
577 Nagata T, Naito YI, Ogawa NO, Popp BN, Steffan S, Takano Y, Tayasu I, Wyatt ASJ, Yamaguchi
578 YT, Yokoyama Y (2017) Advances in the application of amino acid nitrogen isotopic analysis in
579 ecological and biogeochemical studies. Org Geochem 113:150–174. doi:
580 10.1016/j.orggeochem.2017.07.009
581 Phillips DL, Newsome SD, Gregg JW (2005) Combining sources in stable isotope mixing models:
582 Alternative methods. Oecologia 144:520–527. doi: 10.1007/s00442-004-1816-8
583 R Core Team (2020) R: A language and environment for statistical computing. R Foundation for
584 Statistical Computing, Vienna, Austria
585 Rau GH, Sweeney RE, Kaplan IR (1982) Plankton ^{13}C: ^{12}C ratio changes with latitude differences
586 between northern and southern oceans. Deep Sea Res 29:1035–1039.
587 Rodgers KL, Wing SR (2008) Spatial structure and movement of blue cod *Parapercis colias* in Soubtful

588 Sound, New Zealand, inferred from $\delta^{13}C$ and $\delta^{15}N$. Mar Ecol Prog Ser 359:239–248. doi:
589 10.3354/meps07349
590 Schaner T, Patterson WP, Lantry BF, O'Gorman R (2007) Distinguishing wild vs. stocked lake trout
591 (*Salvelinus namaycush*) in Lake Ontario: Evidence from carbon and oxygen stable isotope values of
592 otoliths. J Great Lakes Res 33:912–916. doi: 10.3394/0380-1330(2007)33[912:DWVSLT]2.0.CO;2
593 Schoeninger MJ, DeNiro MJ (1984) Nitrogen and carbon isotopic composition of bone collagen from
594 marine and terrestrial animals. Geochim Cosmochim Acta 48:625–639. doi: 10.1016/0016-
595 7037(84)90091-7
596 Shiao JC, Shirai K, Tanaka K, Takahata N, Sano Y, Sung-Yun Hsiao S, Lee DC, Tseng YC (2018)
597 Assimilation of nitrogen and carbon isotopes from fish diets to otoliths as measured by nanoscale
598 secondary ion mass spectrometry. Rapid Commun Mass Spectrom 32:1250–1256. doi:
599 10.1002/rcm.8171
600 Shigenobu Y, Yoneda M, Kurita Y, Ambe D, Saitoh K (2013) Population subdivision of Japanese
601 flounder *Paralichthys olivaceus* in the Pacific coast of Tohoku Japan detected by means of
602 mitochondrial phylogenetic information. Int J Mol Sci 14:954–963. doi: 10.3390/ijms14010954
603 Sholto-Douglas A, Field J, James A, van der Merwe N (1991) the Southern Benguela Ecosystem:
604 indicators of food web relationships among different size-classes of plankton and pelagic fish;
605 differences between fish muscle and bone collagen tissues. Mar Ecol Prog Ser 78:23–31. doi:

606 10.3354/meps078023

607 Sogawa S, Sugisaki H, Tadokoro K, Ono T, Sato E, Shimode S, Kikuchi T (2017) Feeding habits of six

608 species of euphausiids (Decapoda: Euphausiacea) in the northwestern Pacific Ocean determined by

609 carbon and nitrogen stable isotope ratios. J Crustac Biol 37:29–36. doi: 10.1093/jcbiol/ruw014

610 Tayasu I, Hirasawa R, Ogawa NO, Ohkouchi N, Yamada K (2011) New organic reference materials for

611 carbon- and nitrogen-stable isotope ratio measurements provided by Center for Ecological

612 Research, Kyoto University, and Institute of Biogeosciences, Japan Agency for Marine-Earth

613 Science and Technology. Limnology 12:261–266. doi: 10.1007/s10201-011-0345-5

614 Tomaszewicz CNT, Seminoff JA, Avens L, Kurle CM (2016) Methods for sampling sequential annual

615 bone growth layers for stable isotope analysis. Methods Ecol Evol 7:556–564. doi: 10.1111/2041-

616 210X.12522

617 Tomida Y, Suzuki T, Yamada T, Asami R, Yaegashi H, Iryu Y, Otake T (2014) Differences in oxygen

618 and carbon stable isotope ratios between hatchery and wild pink salmon fry. Fish Sci 80:273–280.

619 doi: 10.1007/s12562-014-0699-9

620 Tomiyama T, Uehara S, Kurita Y (2013) Feeding relationships among fishes in shallow sandy areas in

621 relation to stocking of Japanese flounder. Mar Ecol Prog Ser 479:163–175. doi:

622 10.3354/meps10191

623 Van Klinken GJ (1999) Bone collagen quality indicators for palaeodietary and radiocarbon

624 measurements. J Archaeol Sci 26:687–695. doi: 10.1006/jasc.1998.0385

625 Vanderklift MA, Ponsard S (2003) Sources of variation in consumer-diet δ^{15}N enrichment: A meta-

626 analysis. Oecologia 136:169–182. doi: 10.1007/s00442-003-1270-z

627 Vane K, Wallsgrove NJ, Ekau W, Popp BN (2018) Reconstructing lifetime nitrogen baselines and trophic

628 position of *Cynoscion acoupa* from δ^{15}N values of amino acids in otoliths. Mar Ecol Prog Ser

629 597:1–11.

630 Wada E, Ohki K, Yoshikawa S, Parker PL, Van Baalen C, Matsumoto GI, Aita MN, Saino T (2012)

631 Ecological aspects of carbon and nitrogen isotope ratios of cyanobacteria. Plankt Benthos Res

632 7:135–145. doi: 10.3800/pbr.7.135

633 Wells RD, Kinney MJ, Kohin S, Dewar H, Rooker JR, Snodgrass OE (2015) Natural tracers reveal

634 population structure of albacore (*Thunnus alalunga*) in the eastern North Pacific. ICES J Mar Sci

635 72:2118–2127. doi: 10.1093/icesjms/fst176

636 West JB, Sobek A, Ehleringer JR (2008) A simplified GIS approach to modeling global leaf water

637 isoscapes. PLoS One 3:e2447. doi: 10.1371/journal.pone.0002447

638 Wilson DS (1998) Adaptive individual differences within single populations. Philos Trans R Soc B Biol

639 Sci 353:199–205. doi: 10.1098/rstb.1998.0202

640 Won EJ, Choi B, Lee CH, Hong S, Lee JH, Shin KH (2020) Variability of trophic magnification factors

641 as an effect of estimated trophic position: Application of compound-specific nitrogen isotope

642 analysis of amino acids. Environ Int. doi: 10.1016/j.envint.2019.105361

643 Yamada H, Sato K, Nagahora S, Kumagai A, Yamashita Y (1998) Feeding habits of the Japanese

644 flounder *Paralichthys olivacens* in pacific coastal waters of Tohoku District, Northeastern Japan.

645 Nippon Suisan Gakkaishi 64:249–258. doi: 10.2331/suisan.64.249 (in Japanese with English

646 abstract)

647 Yamamoto M, Tominaga O (2014) Prey availability and daily growth rate of juvenile Japanese flounder

648 *Paralichthys olivaceus* at a sandy beach in the central Seto Inland Sea, Japan. Fish Sci 80:1285–

649 1292. doi: 10.1007/s12562-014-0805-z

650 Yoneda M, Kurita Y, Kitagawa D, Ito M (2007a) Spatial variation in the relationship between growth and

651 maturation rate in male Japanese flounder *Paralichthys olivaceus* off the Pacific coast of northern

652 Japan. J Sea Res 57:171–179. doi: 10.1016/j.seares.2006.08.009

653 Yoneda M, Kurita Y, Kitagawa D, Ito M, Tomiyama T, Goto T, Takahashi K (2007b) Age validation and

654 growth variability of Japanese flounder *Paralichthys olivaceus* off the Pacific coast of northern

655 Japan. Fish Sci 73:585–592. doi: 10.1111/j.1444-2906.2007.01371.x

570 **Table 1.** Summary of analysis of variance of each section of the vertebral centrum of adult *Paralichthys olivaceus*. Different letters denote significant differences ($P < 0.05$) among

571 sampling sites.

(a) $\delta^{13}C_{bulk}$

Site	Vertebral section number																							
	1	2	3	4	5	6	7	8	9	10	11	12	13	14	15	16	17	18	19	20	21	22	23	24
N35	-	a	a	a	a	a	a	a	a	a	a	a	a	a	a	ab	a	a	ab	ab	ab	-	-	-
N55	-	a	a	a	a	a	a	a	a	a	a	a	a	a	a	b	a	a	abc	abc	ab	-	-	-
S30	-	a	a	a	a	a	a	a	a	a	a	a	a	a	a	ab	a	a	c	c	b	-	-	-
S45	-	a	a	a	a	a	a	a	a	a	a	a	a	a	a	a	a	a	a	a	a	-	-	-

(b) $\delta^{15}N_{bulk}$

Site	Vertebral section number

	1	2	3	4	5	6	7	8	9	10	11	12	13	14	15	16	17	18	19	20	21	22	23	24
N35	-	b	b	b	b	b	b	b	b	bc	bc	b	ab	ab	ab	ab	ab	ab	ab	ab	abc	-	-	-
N55	-	a	a	a	a	a	a	a	a	a	a	a	a	a	a	a	a	a	a	a	a	-	-	-
S30	-	b	b	b	b	b	b	b	b	bc	bc	b	bc	bc	bc	bc	bc	bc	bc	bc	c	-	-	-
S45	-	b	b	b	b	b	b	b	b	ab	ab	b	ab	ab	ab	ab	ab	ab	ab	ab	ab	-	-	-

570

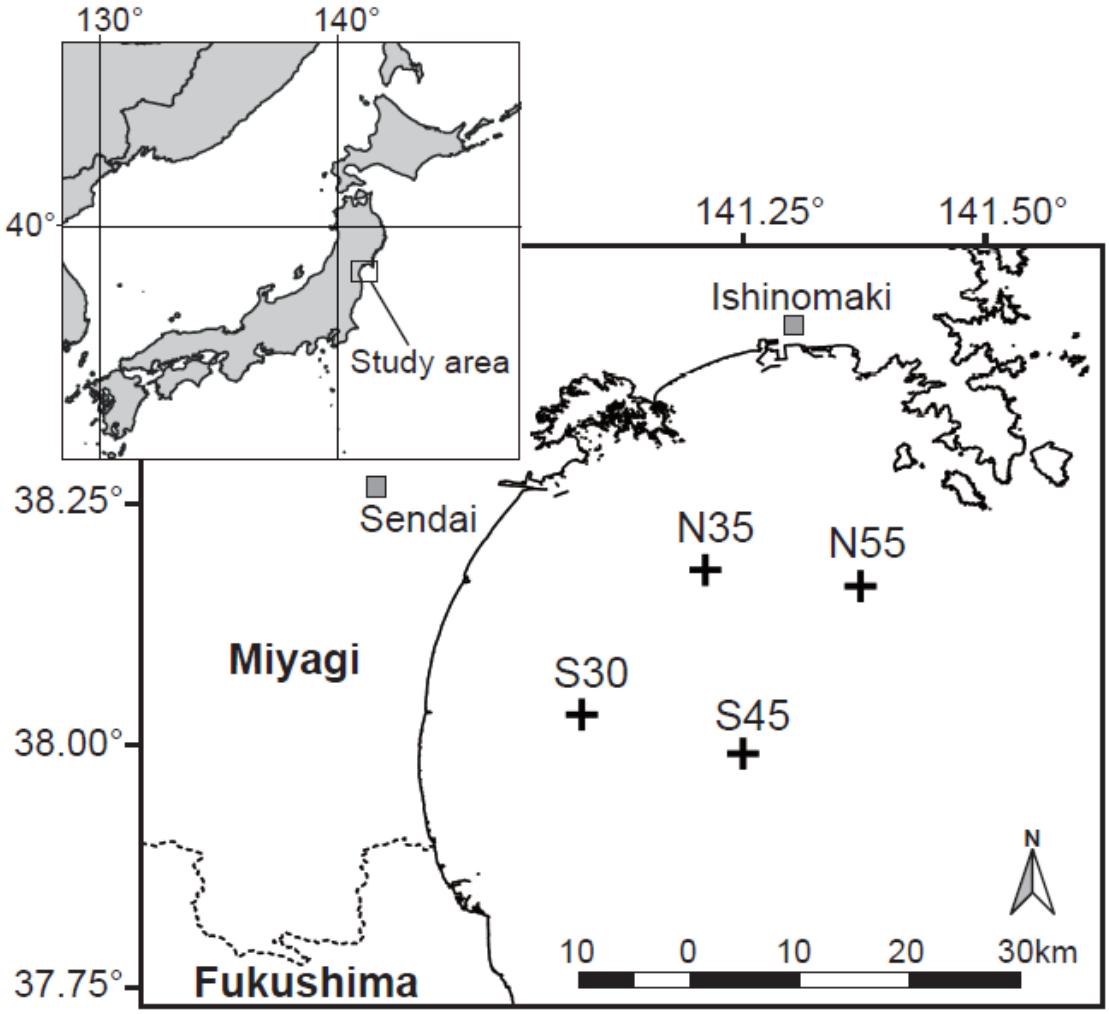

Figure 1. Sampling sites of *Paralichthys olivaceus* in Sendai Bay, Japan. Each number in the name of sampling site indicates approximate water depth (m) of the site. Dotted lines represent the prefectural borders.

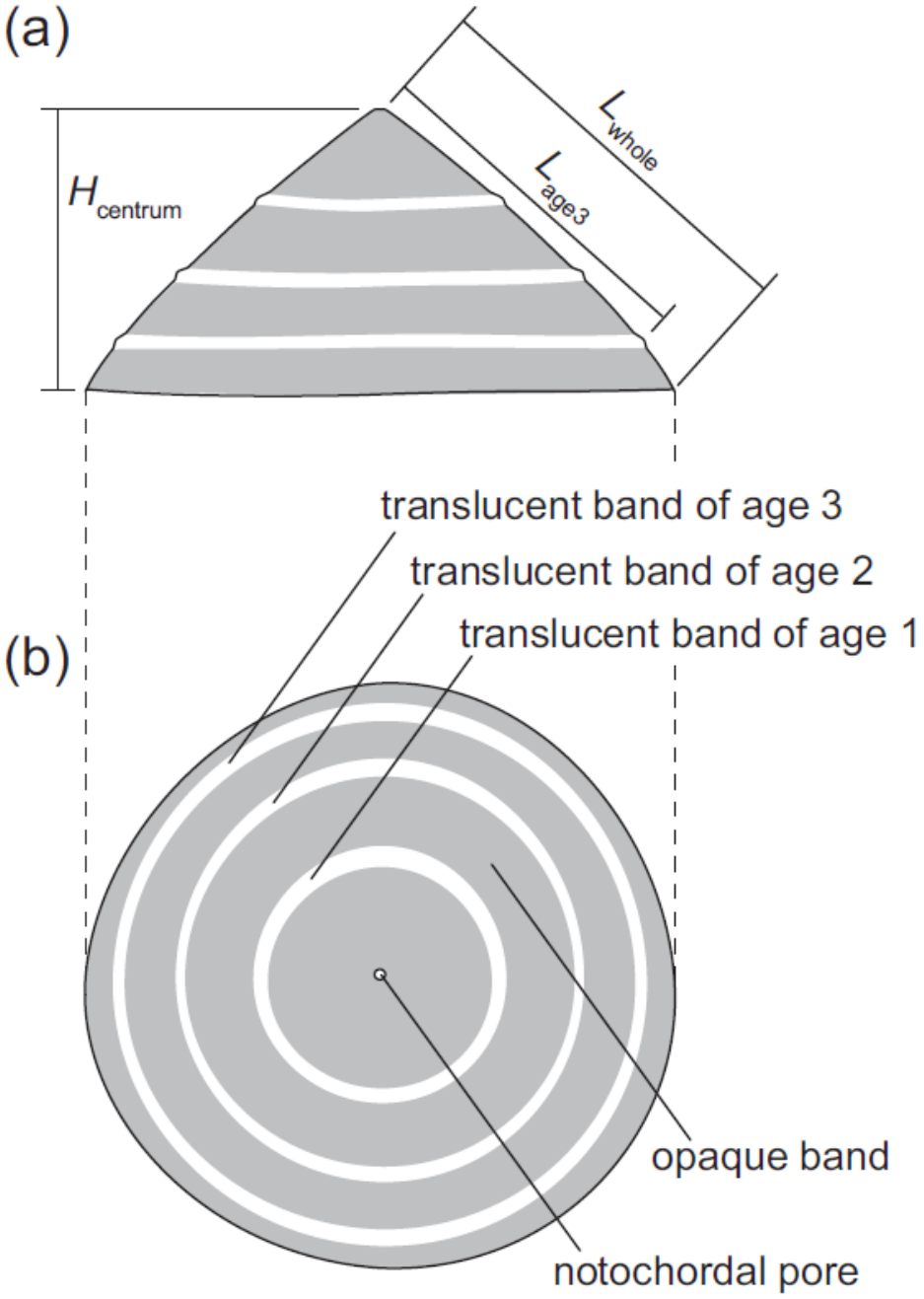

Figure 2. Schematic illustration of single corn in the set of the vertebral centrum of age 3+ *Paralichthys olivaceus*. Images were obtained (**a)** along the craniocaudal axis and (**b)** along the dorsoventral axis. $H_{centrum}$, L_{age3}, and L_{whole} represent the total height of the target centrum, length from the apex to translucent band at age 3, and length from the apex to the outermost edge of the centrum, respectively.

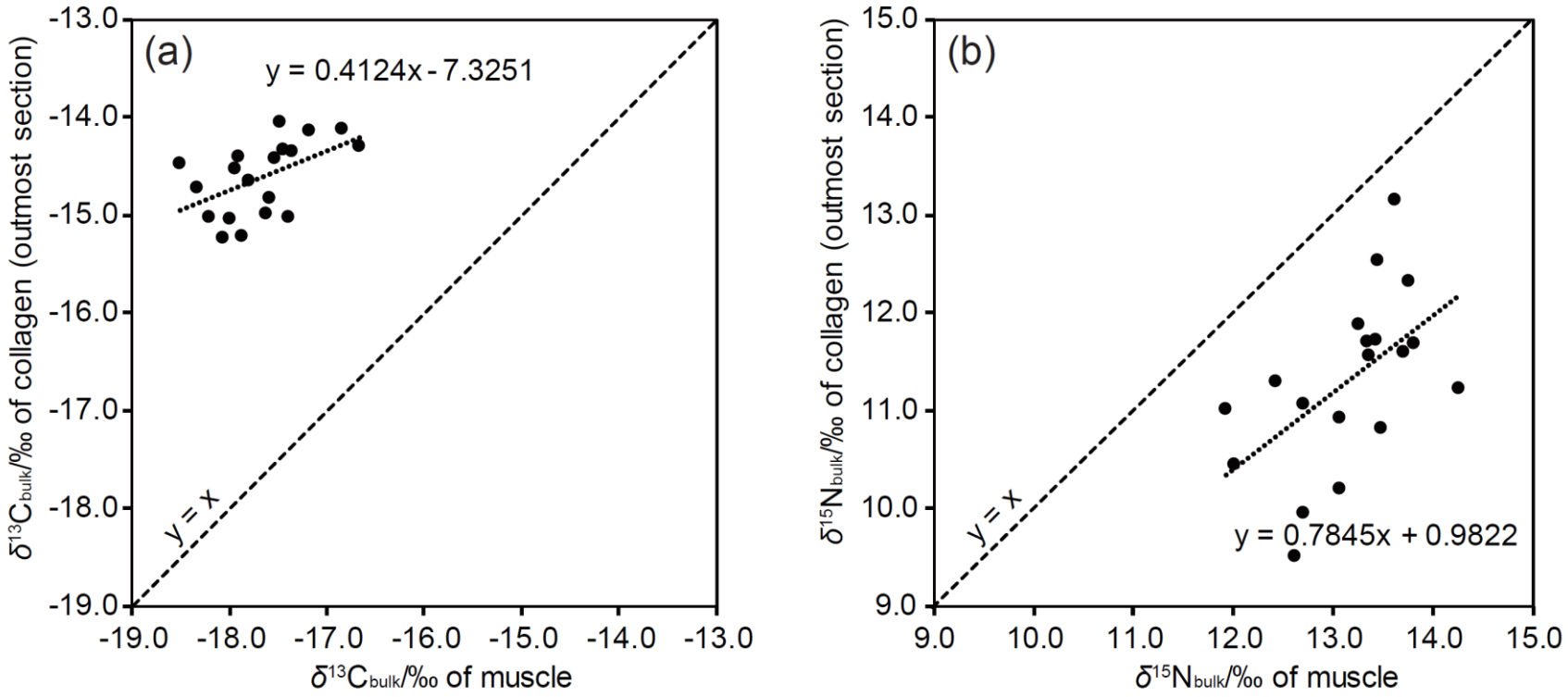

Figure 3. Correlation of stable isotope ratios between muscle and bone collagen in the outermost edge of the vertebral centrum of *Paralichthys olivaceus* in Sendai Bay, Japan: **a** $\delta^{13}C_{bulk}$ values; **b** $\delta^{15}N_{bulk}$ values.

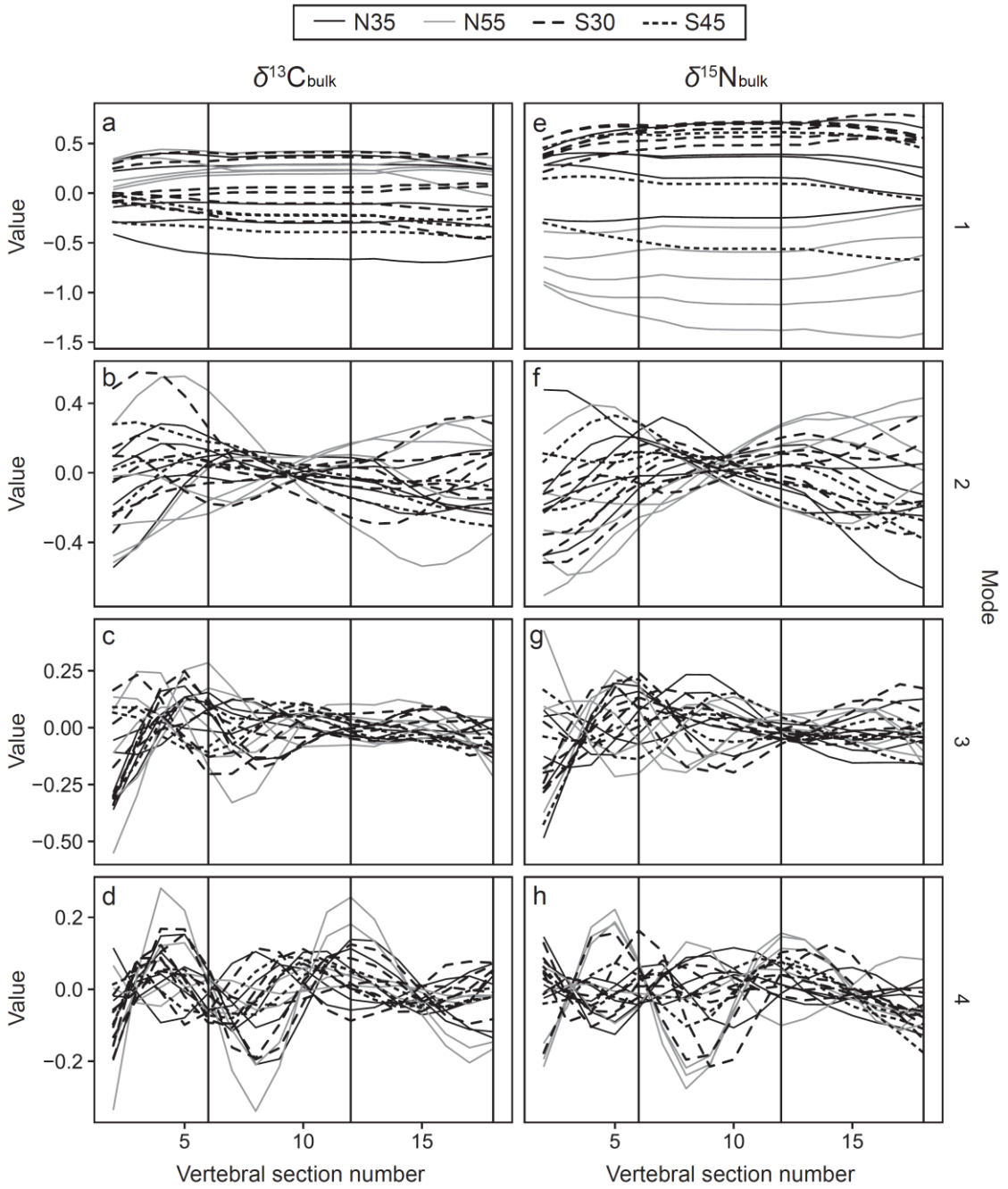

Figure 4. Four modes of variability for $\delta^{13}C_{bulk}$ (a–d) and $\delta^{15}N_{bulk}$ (e–h) of vertebral sectional collagen of *Paralichthys olivaceus* in Sendai Bay, Japan, obtained by nonlinear time-series analysis. Vertical lines show estimated breakpoints between years one, two, and three of individuals (i.e., vertebral section numbers 6,12, and 18).

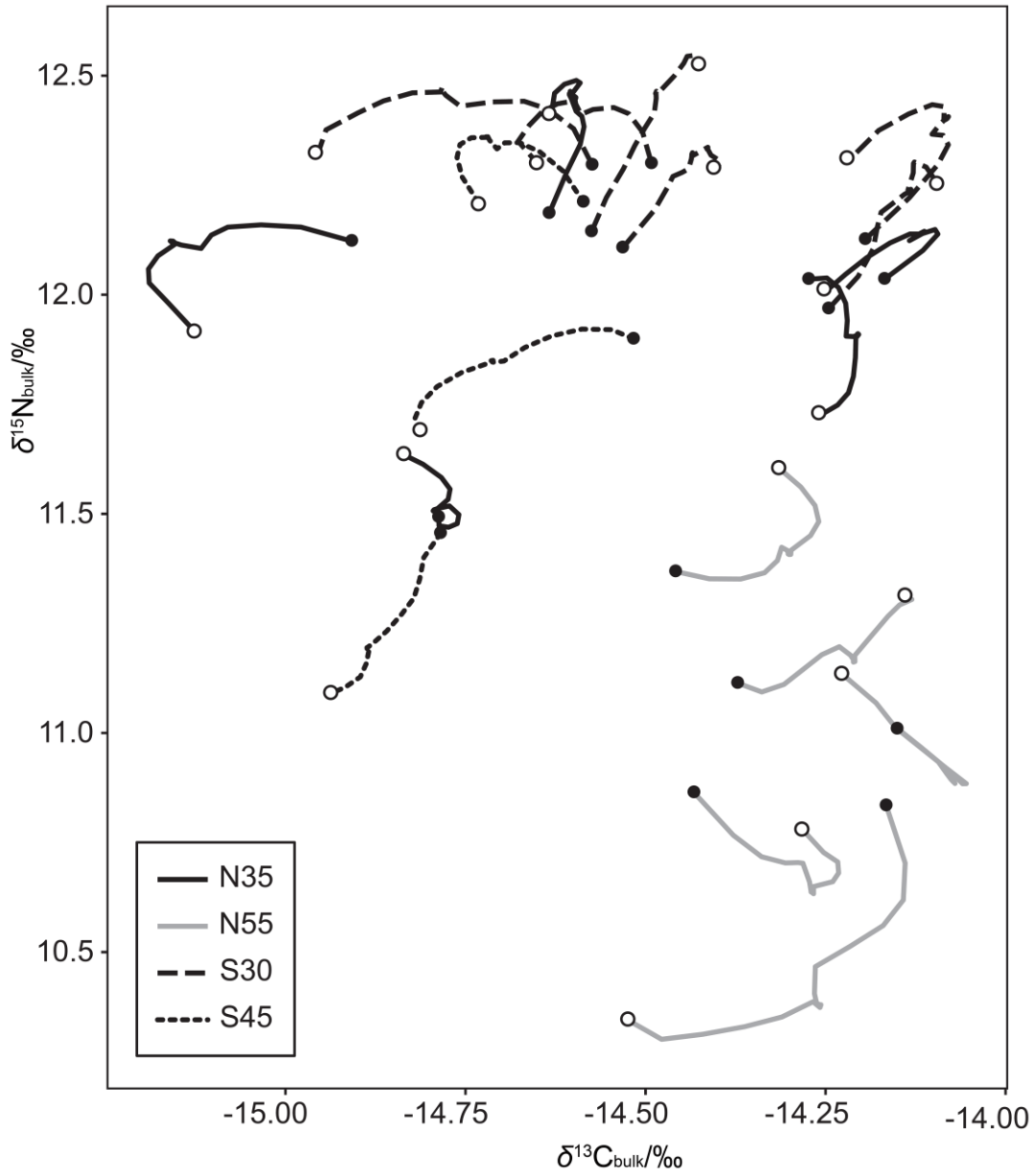

Figure 5. Lifetime transitions of $\delta^{13}C_{bulk}$ and $\delta^{15}N_{bulk}$ values in bone collagen of *Paralichthys olivaceus* in Sendai Bay, Japan, reconstructed by the most salient mode (i.e., mode 1 in Fig. 6) by nonlinear time-series analysis. Filled and open circles indicate the values for the apex and the outermost edge of the vertebral centrum, respectively.

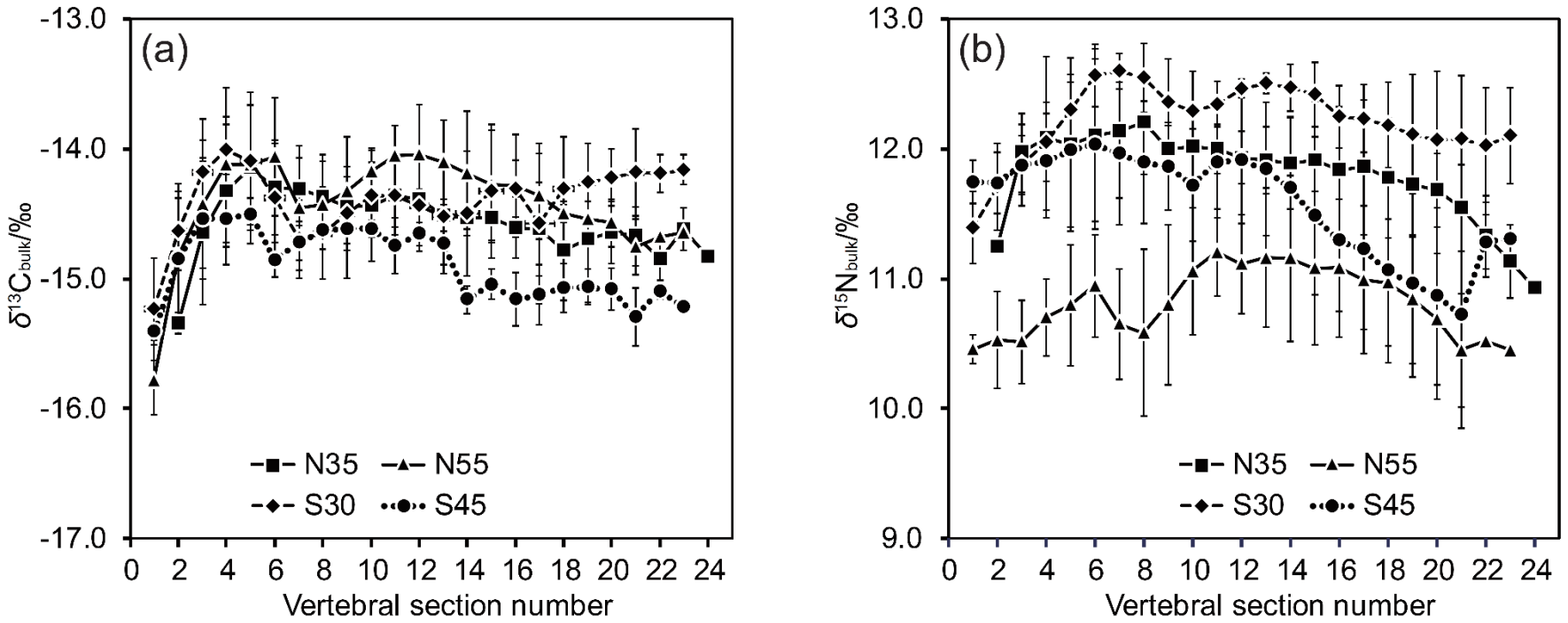

Figure 6. Average and 1σ of stable isotope ratios of vertebral sections from *Paralichthys olivaceus* in Sendai Bay, Japan. Vertebral bone section numbers start at the center of the vertebral centrum and increase toward the margin: **a** $\delta^{13}C_{bulk}$ values; **b** $\delta^{15}N_{bulk}$ values.

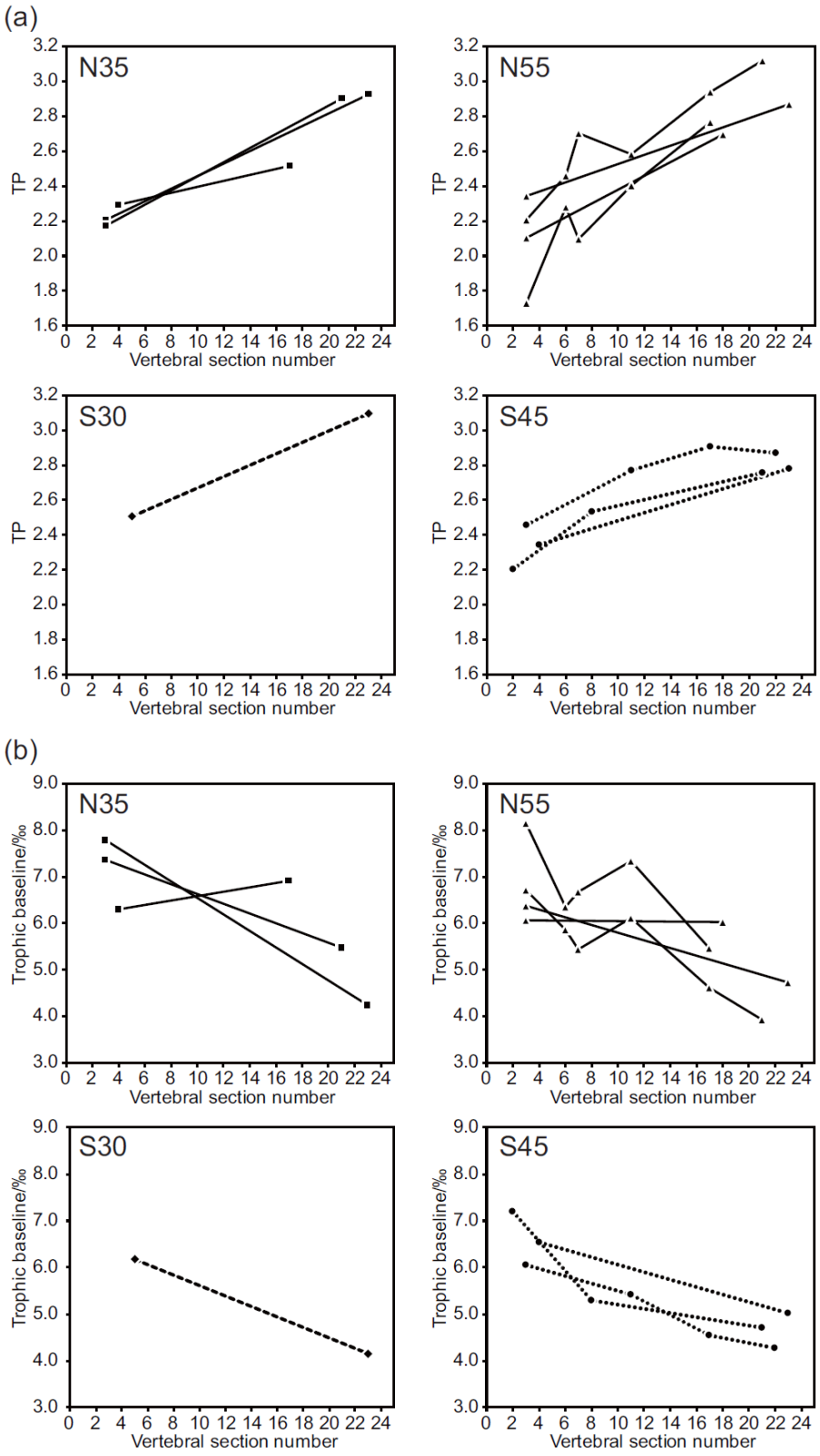

Figure 7. Trophic changes of individual *Paralichthys olivaceus* calculated from δ^{15}N of amino acids: **a**

trophic position; **b** trophic baseline: $\delta^{15}N_{Base}$/‰.